The Astrophysical Journal, 869:26 (5pp), 2018 December 10 https://doi.org/10.3847/1538-4357/aaeb9c

Constraining the Dark Matter Vacuum Energy Interaction Using the EDGES 21 cm Absorption Signal

Yuting Wang[1] and Gong-Bo Zhao[1,2,3]

[1] National Astronomy Observatories, Chinese Academy of Science, Beijing, 100101, People's Republic of China; ytwang@nao.cas.cn

[2] University of Chinese Academy of Sciences, Beijing, 100049, People's Republic of China; gbzhao@nao.cas.cn

[3] Institute of Cosmology and Gravitation, University of Portsmouth, Portsmouth, PO1 3FX, UK

Received 2018 June 12; revised 2018 October 10; accepted 2018 October 23; published 2018 December 7

Abstract

The recent measurement of the global 21 cm absorption signal reported by the Experiment to Detect the Global Epoch of Reionization Signature (EDGES) Collaboration is in tension with the prediction of the ΛCDM model at a 3.8σ significance level. In this work, we report that this tension can be released by introducing an interaction between dark matter and vacuum energy. We perform a model parameter estimation using a combined data set including EDGES and other recent cosmological observations, and find that the EDGES measurement can marginally improve the constraint on parameters that quantify the interacting vacuum, and that the combined data set favors the ΛCDM at a 68% confidence level. This proof-of-concept study demonstrates the potential power of future 21 cm experiments to constrain the interacting dark energy models.

Key words: cosmology: observations – dark energy

1. Introduction

Recently, the Experiment to Detect the Global Epoch of Reionization Signature (EDGES) Collaboration reported an excess 21 cm absorption signal at the effective redshift $z \sim 17$ (Bowman et al. 2018). The amplitude of this observed signal is $T_{21} = -500^{+200}_{-500}$ mK, where the error, including potential systematic uncertainties, is at the 99% confidence level (CL; Bowman et al. 2018). Surprisingly, this measurement is in tension with the theoretical prediction in the standard ΛCDM cosmology at about a 3.8σ significance level, namely, the measured T_{21} almost doubles the ΛCDM prediction, which is $T_{21} = -209$ mK (Barkana 2018).

Much attention from the astrophysics community has been attracted to this discovery, and various interpretations have been proposed to explain the discrepancy. As $T_{21} \propto [1 - T_{\rm CMB}(z)/T_{\rm S}(z)]/H(z)$, where T_{21} is the measured intensity of the 21 cm radiation relative to the cosmic microwave background (CMB) temperature $T_{\rm CMB}(z)$, $T_{\rm S}(z)$ is the spin temperature of the hydrogen gas, and $H(z)$ is the *Hubble* parameter, there are in principle three ways (and their combinations) to make T_{21} more negative to be compatible with the EDGES measurement: (A) reduce the spin temperature $T_{\rm S}$ by introducing new cooling mechanisms, e.g., the dark matter-baryon scattering (Barkana 2018; Berlin et al. 2018; Fialkov et al. 2018; Muñoz & Loeb 2018), (B) raise $T_{\rm CMB}$ by additional radio background (Ewall-Wice et al. 2018; Feng & Holder 2018; Fraser et al. 2018), or (C) reduce the *Hubble* parameter (Costa et al. 2018; Hill & Baxter 2018).

In this paper, we propose to release the tension by reducing the *Hubble* parameter through the interaction between dark matter and dark energy. Specifically, we consider the interacting vacuum energy model[4] proposed in Wands et al. (2012), and perform a parameter estimation for this model using a joint data set including EDGES and other kinds of recent cosmological measurements.

This paper is organized as follows. In the next section, we present a brief description of the 21 cm absorption observable. Then we introduce the interacting vacuum energy model in Section 3, before showing the cosmological constraint on the interacting vacuum energy model using observations in Section 4. The last section is devoted to a conclusion and discussions.

2. The 21 cm Absorption Signal

At the Rayleigh–Jeans limit, the brightness temperature of the observed radiation field is (Field 1958; Furlanetto et al. 2006),

$$T_b(z, \nu) = T_{\rm CMB}(z)e^{-\tau_\nu} + T_{\rm S}(z)(1 - e^{-\tau_\nu}), \quad (1)$$

where z and ν denote redshift and frequency, respectively, and τ_ν is the optical depth of the inter-galactic medium at frequency ν. $T_S(z)$ is the spin temperature, and $T_{\rm CMB}$ is the CMB temperature which evolves with redshift as $T_{\rm CMB}(z) = 2.725(1 + z)$ K.

The 21 cm signal is caused by the hyperfine splitting of neutral hydrogen atoms. The transition from the triplet state to the singlet state corresponds to the emission of photons of wavelength at 21 cm, whose frequency is $\nu_0 = 1420.4$ MHz. The intensity of the 21 cm radiation relative to the CMB temperature is thus

$$T_{21}(z) \approx \frac{T_{\rm S}(z) - T_{\rm CMB}(z)}{1 + z}\tau_{\nu_0}(z), \quad (2)$$

$$\tau_{\nu_0}(z) = \frac{2c^3\hbar A_{10} n_{\rm H\,I}}{16 k_{\rm B}\nu_0^2 T_{\rm S}(z)H(z)}, \quad (3)$$

where c is the speed of light, $\hbar$ the reduced Planck constant, and $k_{\rm B}$ the Boltzmann constant. $A_{10} = 2.85 \times 10^{-15}\,{\rm s}^{-1}$ is the emission coefficient of the spontaneous transition from the triplet state to the singlet state. $n_{\rm H\,I}$ is the number density of neutral hydrogen, and $H(z)$ is the *Hubble* parameter as a

[4] The idea of decaying vacuum energy is a recurring concept to explain the accelerating expansion of the universe (Bertolami 1986; Freese et al. 1987; Chen & Wu 1990; Carvalho et al. 1992; Berman 1991; Pavon 1991; Al-Rawaf & Taha 1996; Shapiro & Solà 2002; Solà 2011).

function of redshift. In ΛCDM, $H(z)$ can be approximated as $H_0\sqrt{\Omega_{\rm M}(1+z)^3}$ at $z \gg 1$, such that the optical depth in Equation (3) can be rewritten as (Furlanetto et al. 2006)

$$\tau_{\nu_0}^{\Lambda{\rm CDM}} \approx 8.6 \times 10^{-3} x_{HI}\left[\frac{T_{\rm CMB}(z)}{T_{\rm S}(z)}\right]\left(\frac{\Omega_b h^2}{0.02}\right) \times \left[\left(\frac{0.15}{\Omega_{\rm M}h^2}\right)\left(\frac{1+z}{10}\right)\right]^{1/2}, \quad (4)$$

where $x_{\rm H\,I}$ is the neutral hydrogen fraction, and $\Omega_b h^2$ and $\Omega_{\rm M}h^2$ are the physical baryon and matter densities, respectively.

3. The Interacting Vacuum Energy Model

With the presence of the interacting vacuum energy, the continuity equations for the interacting vacuum V and dark matter $\rho_{\rm dm}$ are

$$\dot{V} = Q, \qquad \dot{\rho}_{\rm dm} + 3H\rho_{\rm dm} = -Q, \quad (5)$$

where Q is the interaction between the vacuum energy and dark matter. Vacuum energy has a non-varying equation of state, i.e., $w \equiv -1$, but a time-evolving energy density due to the interacting term Q, which is different from the interacting dark energy models discussed in Costa et al. (2018), where the equation of state of dark energy is a constant w, but $w \neq -1$. In this work, we consider an interaction of the form

$$Q = 3\alpha H \frac{\rho_{\rm dm} V}{\rho_{\rm dm} + V}. \quad (6)$$

Note that α can be a function of time in general. In this work, we parameterize the time-dependence as

$$\alpha(a) = \alpha_0 + \alpha_a(1-a). \quad (7)$$

As shown, α approaches α_0 and $\alpha_0 + \alpha_a$ in limits of $a = 1$ and $a = 0$, respectively, and interpolates linearly in between. In this model, $\alpha_a = -d\alpha/da$, thus it can be used as an indicator of the dynamics of the vacuum. The effective equation of state for vacuum energy is

$$w_V^{\rm eff} = -1 - \alpha(a)\frac{\rho_{\rm dm}}{\rho_{\rm dm} + V}. \quad (8)$$

This parametrization of $\alpha(a)$ can realize a quintom-like effective dark energy with the equation of state crossing -1, as shown in the upper left and the lower right regions of Figure 1. In contrast, a constant interaction parameter, i.e., $\alpha(a) = \alpha_0$ discussed in Wang et al. (2013, 2014), can only yield a quintessence-like dark energy with $w_V^{\rm eff} > -1$ for a negative α_0 or a phantom-like dark energy with $w_V^{\rm eff} < -1$ for a positive α_0.

The Friedmann equation reads as

$$H^2 = \frac{8\pi G}{3}[\rho_b + \rho_r + \rho_{\rm dm} + V], \quad (9)$$

where baryons and radiation follow the standard conservation equations. The expansion history of the universe can be solved by combining Equations (5), (6), (7), and (9). Apparently, any non-zero α yields a modification of expansion history compared with that in the ΛCDM model (Wang et al. 2013). As the 21 cm temperature T_{21} depends on $\tau_{\nu 0}$, which further depends on the expansion rate H through Equation (3), the interacting vacuum model can leave imprints on the 21 cm observables.

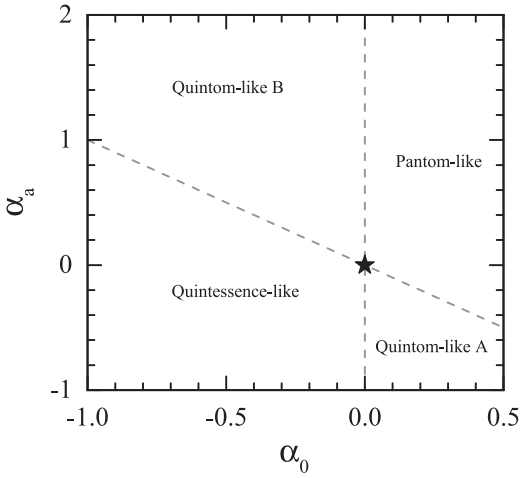

Figure 1. Dashed lines of $\alpha_0 = 0$ and $\alpha_0 + \alpha_a = 0$ divide the parameter space of α_0 and α_a into four regions, where $w_V^{\rm eff}$ is greater than -1 in the past and smaller than -1 today in the models of quintom-like A, while $w_V^{\rm eff}$ crosses -1 from the values smaller than -1 to that greater than -1 in the models of quintom-like B. The black star denotes the ΛCDM model.

At the perturbation level, we consider an energy flow that is parallel to the 4-velocity of dark matter, i.e., $Q^\mu_{\rm dm} = -Qu^\mu_{\rm dm}$. In this case dark matter particles follow geodesics as in ΛCDM, but the continuity equation gets modified, namely, the velocity perturbation for dark matter is not affected by the interaction and obeys the standard equation (Wang et al. 2013, 2014)

$$\dot{\theta}_{\rm dm} = 0. \quad (10)$$

Thus we will evolve the perturbation equations in a synchronous gauge that is comoving with the dark matter.[5] Meanwhile, the dark matter density contrast $\delta_{\rm dm}$ evolves in the dark matter-comoving frame (Wang et al. 2013, 2014),

$$\dot{\delta}_{\rm dm} = -\frac{\dot{h}}{2} + \frac{Q}{\rho_{\rm dm}}\delta_{\rm dm}, \quad (11)$$

where h is the scalar mode of metric perturbations in the synchronous gauge. In this gauge, the vacuum energy is spatially homogeneous, i.e., $\delta V = 0$.

4. Observational Constraints

We use a modified version of Code for Anisotropies in the Microwave Background (CAMB; Lewis et al. 2000)[6] to compute the theoretical prediction of $T_{21}(z)$ using Equations (2)–(9), given a set of cosmological parameters,

$$P \equiv \{\omega_b, \omega_c, \Theta_s, \tau, n_s, A_s, \alpha_0, \alpha_a\}, \quad (12)$$

where ω_b and ω_c are the physical baryon and cold dark matter densities, respectively, Θ_s is 100 times the ratio of the sound horizon to the angular diameter distance at decoupling, τ is the reionization optical depth, n_s and A_s are the spectral index and the amplitude of the primordial power spectrum, respectively,

[5] If the initial value of $\theta_{\rm dm}$ is set to zero, it would remain zero at all times.
[6] Available at https://camb.info.

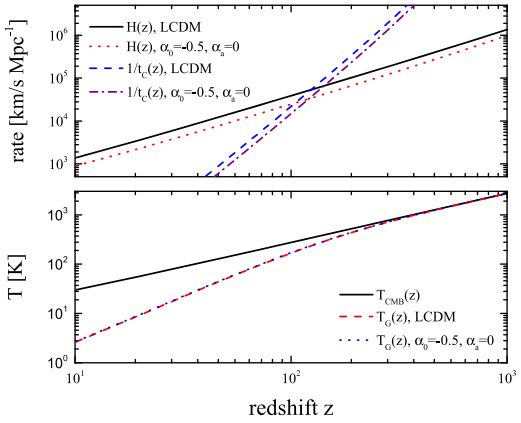

Figure 2. Upper panel: the cosmic expansion rate and Compton-heating rate in the ΛCDM and the interacting vacuum energy model with fixed parameters, i.e., $\alpha_0 = -0.5$ and $\alpha_a = 0$. Lower panel: CMB temperature and gas temperatures in the ΛCDM and the interacting vacuum energy model with fixed parameters, i.e., $\alpha_0 = -0.5$ and $\alpha_a = 0$.

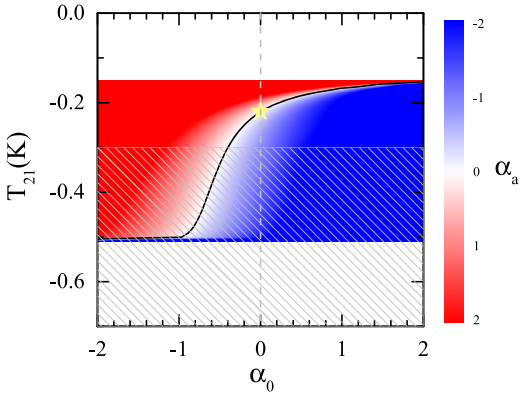

Figure 3. Illustration of the intensity of the 21 cm signal relative to the CMB temperature, T_{21} (K), for various values of α_0 and α_a. The color bar indicates the values of α_a. The black solid curve corresponds to the case in which α does not evolve with time ($\alpha_a = 0$). The intersect between the black solid curve and the vertical gray dashed line, marked by a yellow star, denotes the ΛCDM model. The hatched region illustrates the observed 21 cm signal from EDGES at a 99% CL.

and α_0 and α_a parameterize the strength of the interacting vacuum in the form of Equation (7).

It is assumed that the spin temperature $T_S(z)$ fully couples to the gas temperature $T_G(z)$ at redshifts of $z \simeq 15$–20, as indicated by the observed 21 cm signal from EDGES, and as discussed in recent paper (Xiao et al. 2018), and we compute the evolution of $T_G(z)$ using RECFAST (Seager et al. 1999, 2000; Wong et al. 2008; Scott & Moss 2009).[7] The evolution equation of the gas temperature $T_G(z)$ is given in Seager et al. (1999) and in Scott & Moss (2009), i.e.,

$$\frac{dT_G(z)}{dz} = \frac{T_G(z) - T_{CMB}(z)}{H(z)(1+z)t_C(z)} + \frac{2T_G(z)}{1+z}, \quad (13)$$

where $t_C(z)$ is the Compton-heating timescale, i.e.,

$$t_C(z) = \frac{3m_e c}{8\sigma_T a_R T_{CMB}^4(z)}\left[\frac{1+f_{He}(z)+x_e(z)}{x_e(z)}\right]. \quad (14)$$

Here m_e is the electron mass, c is the speed of light, σ_T is the Thomson scattering cross section, a_R is the radiation constant, $f_{He}(z)$ is the fractional abundance of helium by number, and $x_e(z)$ is the free electron fraction normalized to the total hydrogen number density. The decoupling time between gas and CMB is at $H \approx 1/t_C(z)$.

As shown in Equation (13), the evolution of the gas temperature also depends on $H(z)$. In order to figure out the effect of $H(z)$ on the EDGES signal, we show the cosmic expansion rate $H(z)$ and Compton-heating rate $1/t_C(z)$ in the ΛCDM and the interacting vacuum energy model with fixed parameters, i.e., $\alpha_0 = -0.5$ and $\alpha_a = 0$ in the upper panel of Figure 2. It is seen that the interacting vacuum model has a smaller $H(z)$, but the decoupling time between gas and CMB at which $H \approx 1/t_C(z)$ in the interacting vacuum energy model has very little change, compared with that in ΛCDM. In the lower panel of Figure 2, we show the CMB temperature and gas temperatures in the ΛCDM and interacting vacuum energy model with fixed parameters, i.e., $\alpha_0 = -0.5$ and $\alpha_a = 0$. Both models have very close gas temperatures. Therefore, according to Equation (2) we can see that a reduced value of $H(z)$ in Equation (3) would be the main contribution to an increase of the amplitude of the 21 cm signal.

In Figure 3, we show T_{21}, as defined in Equation (2), for various values of α_0 and α_a, with other cosmological parameters fixed at values consistent with a Planck 2015 cosmology (Planck Collaboration et al. 2016). As shown, the ΛCDM model ($\alpha_0 = \alpha_a = 0$), denoted by the star, is in tension with the EDGES measurement at a 99% CL illustrated by the hatched region. However, interacting vacuum models can in principle release the tension, namely, T_{21} can be pushed into the hatched region by a large range of the α_0 and α_a parameters.

We then perform a Monte Carlo Markov Chain global fit for the parameters in Equation (12) using a modified version of CosmoMC[8] (Lewis & Bridle 2002) with a combined data set including,

1. the angular power spectra of temperature and polarization measurements of CMB from the Planck mission (Planck Collaboration et al. 2016);
2. the Joint Light-curve Analysis sample of supernovae (SNe) measurements (Betoule et al. 2014);
3. the Baryonic Acoustic Oscillations (BAO) distance measurements from 6dFGS (Beutler et al. 2011), Sloan Digital Sky Survey (SDSS) DR7 Main Galaxy Sample (Ross et al. 2015), Lyα forest of BOSS DR11 quasars (Font-Ribera et al. 2014; Delubac et al. 2015), and BOSS DR12 with tomographic information (Wang et al. 2017; Zhao et al. 2017); joint BAO and Redshift Space Distortions (RSD) measurements from WiggleZ (Blake et al. 2012) and from eBOSS DR14 (Zhao et al. 2019); and RSD measurements from 6dFGS (Beutler et al. 2012), 2dFGRS (Percival et al. 2004), SDSS LRG (Samushia et al. 2012), and VIPERS (de la Torre et al. 2013);
4. and the local H_0 measurement using the Cepheids, i.e., $H_0 = 73.24 \pm 1.74\,\mathrm{km\,s^{-1}\,Mpc^{-1}}$ (Riess et al. 2016).

The results are summarized in Table 1 and in Figures 4 and 5. To quantify the constraint on α_0 and α_a from the EDEGS measurement, we show the 68%, 95%, and 99% CL contours of

[7] Available at http://www.astro.ubc.ca/people/scott/recfast.html.

[8] Available at https://cosmologist.info/cosmomc/.

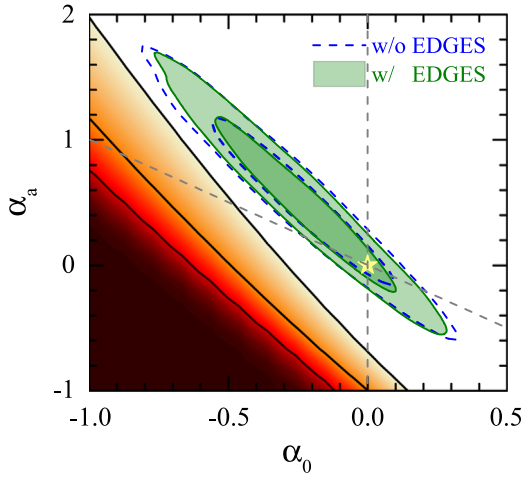

Figure 4. Contour plots for the parameters $\{\alpha_0, \alpha_a\}$ derived from different data combinations including EDGES alone (shaded regions and solid curves in the left corner; the solid curves from left to right denote the 68%, 95%, and 99% CL contours, respectively), CMB + SNe + BAO + RSD + H_0 (blue dashed), and CMB + SNe + BAO + RSD + H_0 + EDGES (solid green). The yellow star marks the ΛCDM model. The dashed lines denote $\alpha_0 = 0$ and $\alpha_0 + \alpha_a = 0$, which divide the α_0–α_a parameter space into four regions, as illustrated in Figure 1.

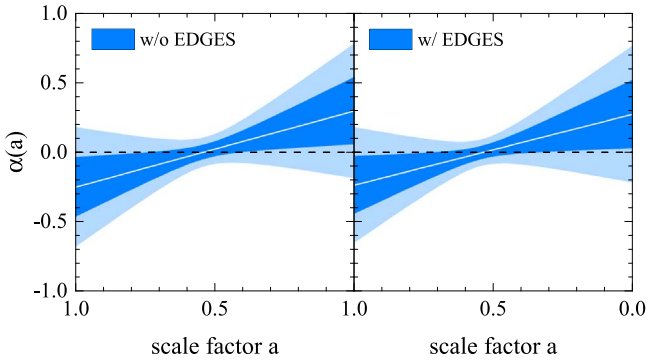

Figure 5. 68% and 95% CL parametric reconstruction of $\alpha(a)$ using CMB+SNe+BAO+RSD+H_0 with (right) and without (left) the EDGES measurement.

Table 1
Mean and 68% CL Constraints on Parameters for Interacting Vacuum (with All Other Relevant Parameters Marginalized Over) Using the Combined Data Sets of CMB, SNe, BAO, RSD, and H_0 with or without the EDGES Measurement

	CMB+SNe+BAO+RSD+H_0	
	Without EDGES	With EDGES
α_0	-0.252 ± 0.216	-0.237 ± 0.208
α_a	0.547 ± 0.446	0.510 ± 0.445
Figure of Merit	1	1.1

Note. The last row shows the figure of merit for α_0 and α_a (the case without EDGES is normalized to 1).

α_0 and α_a using EDEGS alone in the lower left part of Figure 4.[9] As illustrated, the EDGES measurement favors an interacting vacuum model over the ΛCDM model at more than 99% CL, and this would induce a quintessence-like effective dark energy as shown in the lower left of Figure 1. We then perform a global fit for all parameters in Equation (12) using the abovementioned joint data set with and without the EDEGS measurement, and show the 68% and 95% CL contours of $\alpha 0$ and α_a in Figure 4. As we can see, the EDGES data make the contours shrink marginally without changing the degeneracy between α_0 and α_a, namely, the error bars of α_0 and α_a are tightened by 4% and 0.2%, respectively, and the figure of merit, which is the determinant of the inverse covariance matrix for α_0 and α_a, gets improved by 10%, as shown in Table 1. The ΛCDM model is compatible with data within a 68% CL in both cases. This is expected as the comparatively low precision of the EDGES measurement makes it difficult to compete with the remaining combined data sets.

To see the evolution history of α allowed by current observations, we reconstruct $\alpha(a)$ using the constraint that we derived with the functional form assumed in the first place, and show the result in Figure 5. As expected, adding the EDGES data barely changes the reconstruction, and a sweet spot, the epoch at which the error of α gets minimized, shows up at $a \sim 0.5$ ($z \sim 1$) in both cases, and at this epoch, the best-fit value of α changes sign, i.e., energy transfers from dark matter to vacuum energy at early times ($z \gtrsim 1$) and vice versa at late times ($z \lesssim 1$).

5. Conclusion

The recent measurement of the 21 cm brightness temperature performed by the EDGES team has attracted wide attention, partially due to the fact that the observed signal is far below what is expected in a ΛCDM model. Interpretations have been proposed, and most of which focus on the nature of dark matter.

In this work, we perform a proof-of-concept study of the potential power of 21 cm measurements to constrain the possible interaction between dark matter and dark energy. We find that EDGES alone can yield a non-trivial constraint on $\alpha 0$ and α_a parameters quantifying the interaction (with all other parameters fixed), and an interaction vacuum model is able to explain the measured 21 cm brightness temperature.

Given the large uncertainty in the current EDGES measurement, it marginally improves the constraint on α_0 and α_a on top of a compilation of recent measurements of SNe, CMB, BAO, and RSD, and the ΛCDM model agrees with the combined data sets within a 68% CL. An improved test will benefit from more realistic systematic uncertainties in the future. Additionally, future 21 cm measurements, such as the square kilometer array,[10] will provide a much more precise measurement on α, which offers a new probe to shed light on the nature of dark energy and dark matter.

The authors thank Bin Yue and Xuelei Chen for discussions. The authors also thank David Wands for discussions and comments. Y.W. and G.B.Z. are supported by NSFC grants 1171001024 and 11673025. G.B.Z. is also supported by the National Key Basic Research and Development Program of China (No. 2018YFA0404503) and a Royal Society Newton Advanced Fellowship, hosted by University of Portsmouth. Y.W. is also supported by the Nebula Talents Program of NAOC and the Young Researcher Grant of NAOC. This

[9] As EDEGS alone cannot constrain all of the parameters in Equation (12) simultaneously, we only vary α_0 and α_a in this case while the other parameters are fixed to the values derived from the Planck 2015 measurement.

[10] More information is available at https://www.skatelescope.org/.

research used resources of the SCIAMA cluster supported by University of Portsmouth, and the ZEN cluster supported by NAOC.

ORCID iDs

Yuting Wang https://orcid.org/0000-0001-7756-8479
Gong-Bo Zhao https://orcid.org/0000-0003-4726-6714

References

Al-Rawaf, A. S., & Taha, M. O. 1996, PhLB, 366, 69
Barkana, R. 2018, Natur, 555, 71
Berlin, A., Hooper, D., Krnjaic, G., & McDermott, S. D. 2018, PhRvL, 121, 011102
Berman, M. S. 1991, PhRvD, 43, 1075
Bertolami, O. 1986, NCimB, 93, 36
Betoule, M., Kessler, R., Guy, J., et al. 2014, A&A, 568, A22
Beutler, F., Blake, C., Colless, M., et al. 2011, MNRAS, 416, 3017
Beutler, F., Blake, C., Colless, M., et al. 2012, MNRAS, 423, 3430
Blake, C., Brough, S., Colless, M., et al. 2012, MNRAS, 425, 405
Bowman, J. D., Rogers, A. E. E., Monsalve, R. A., et al. 2018, Natur, 555, 67
Carvalho, J. C., Lima, J. A. S., & Waga, I. 1992, PhRvD, 46, 2404
Chen, W., & Wu, Y. S. 1990, PhRvD, 41, 695
Costa, A. A., Landim, R. C. G., Wang, B., & Abdalla, E. 2018, EPJC, 78, 746
de la Torre, S., Guzzo, L., Peacock, J. A., et al. 2013, A&A, 557, A54
Delubac, T., Bautista, J. E., Busca, N. G., et al. 2015, A&A, 574, A59
Ewall-Wice, A., Chang, T.-C., Lazio, J., et al. 2018, ApJ, 868, 63
Feng, C., & Holder, G. 2018, ApJL, 858, L17
Fialkov, A., Barkana, R., & Cohen, A. 2018, PhRvL, 121, 011101
Field, G. B. 1958, PIRE, 46, 240
Font-Ribera, A., Kirkby, D., Busca, N., et al. 2014, JCAP, 5, 027
Fraser, S., Hektor, A., Hütsi, G., et al. 2018, PhLB, 785, 159
Freese, K., Adams, F. C., Frieman, J. A., & Mottola, E. 1987, NuPhB, 287, 797
Furlanetto, S. R., Oh, S. P., & Briggs, F. H. 2006, PhR, 433, 181
Hill, J. C., & Baxter, E. J. 2018, JCAP, 8, 037
Lewis, A., & Bridle, S. 2002, PhRvD, 66, 103511
Lewis, A., Challinor, A., & Lasenby, A. 2000, ApJ, 538, 473
Muñoz, J. B., & Loeb, A. 2018, Natur, 557, 684
Pavon, D. 1991, PhRvD, 43, 375
Percival, W. J., Burkey, D., Heavens, A., et al. 2004, MNRAS, 353, 1201
Planck Collaboration, Ade, P. A. R., Aghanim, N., et al. 2016, A&A, 594, A13
Planck Collaboration, Aghanim, N., Arnaud, M., et al. 2016, A&A, 594, A11
Riess, A. G., Macri, L. M., Hoffmann, S. L., et al. 2016, ApJ, 826, 56
Ross, A. J., Samushia, L., Howlett, C., et al. 2015, MNRAS, 449, 835
Samushia, L., Percival, W. J., & Raccanelli, A. 2012, MNRAS, 420, 2102
Scott, D., & Moss, A. 2009, MNRAS, 397, 445
Seager, S., Sasselov, D. D., & Scott, D. 1999, ApJL, 523, L1
Seager, S., Sasselov, D. D., & Scott, D. 2000, ApJS, 128, 407
Shapiro, I. L., & Solà, J. 2002, JHEP, 2, 006
Solà, J. 2011, J Phys.: Conf. Ser., 283, 012033
Wands, D., De-Santiago, J., & Wang, Y. 2012, CQGra, 29, 145017
Wang, Y., Wands, D., Xu, L., De-Santiago, J., & Hojjati, A. 2013, PhRvD, 87, 083503
Wang, Y., Wands, D., Zhao, G.-B., & Xu, L. 2014, PhRvD, 90, 023502
Wang, Y., Zhao, G.-B., Chuang, C.-H., et al. 2017, MNRAS, 469, 3762
Wong, W. Y., Moss, A., & Scott, D. 2008, MNRAS, 386, 1023
Xiao, L.-F., An, R., Zhang, L., et al. 2018, arXiv:1807.05541
Zhao, G.-B., Wang, Y., Saito, S., et al. 2017, MNRAS, 466, 762
Zhao, G.-B., Wang, Y., Saito, S., et al. 2019, MNRAS, 482, 3497